Charge-Displacement Analysis as a Tool to Study Chalcogen Bonded Adducts and Predict their Association Constants in Solution[†]

Gianluca Ciancaleoni,[a]* Claudio Santi,[b] Mirco Ragni,[c] Antonio Luiz Braga[a]

[a] Departamento de Química, Universidade Federal de Santa Catarina, 88040-900 Florianópolis, SC, Brazil

[b] Dipartimento di Scienze Farmaceutiche, Università di Perugia, Via del Liceo 1, 06134, Perugia, Italy

[c] Departamento de Física, Universidade Estadual de Feira de Santana, 44036-900 Feira de Santana, BA, Brazil

[†] **Electronic Supplementary Information (ESI) available**. Additional tables and figures.

Abstract

The secondary interaction between a polarized atom of tellurium and different Lewis bases, either anionic and neutral, has been studied by Charge Displacement analysis. Through the latter, the charge rearrangement in the adduct upon the formation of the interaction has been quantified and described in great detail. Comparing theoretical results with the experimental association constants, two linear correlations can be found, for anionic and neutral bases, respectively. Such correlations can be used to reliably predict the association constant of adducts for which experimental data are not available yet.

Introduction

Secondary bonding interactions (SBI)[1] play a crucial role in chemistry and biochemistry. During the last decades a special attention has been paid to the intramolecular and intermolecular contacts between di- and tetracoordinate sulfur, selenium, and tellurium atoms and oxygen, nitrogen, sulfur

atoms[2] and even π systems.[3] Any time these interatomic contacts result to be longer than covalent single bond but shorter than the sum of the corresponding van der Waals radii, the presence of a secondary bond is supposed to exist (the interaction is often referred to as chalcogen bond,[4] ChB), often determining a peculiar conformation of the molecules and influencing their reactivity.[5] The presence of this interaction has been demonstrated by solid state experimental data[2,6] and confirmed in solution by spectroscopic evidences.[7,8]

SBIs are fundamental in determining the tridimensional structure of inorganic materials and macromolecules, like secondary and tertiary structures of proteins and biopolymers.[9] Beside the most conventional hydrogen bonding, the investigation of some biopolymers and organic conductors evidenced the role of less conventional interactions, such as those between chalcogen centers, demonstrating their ability on promoting the conformational stabilization.[10]

Furthermore, close contacts between nucleophilic sites and electron-deficient covalent-bonded chalcogens have been supposed to be responsible of the enantioselectivity showed by some chalcogen-containing electrophilic reagents in a number of addition reactions to carbon-carbon double bond, both in inter- and intramolecular processes. It was unequivocally demonstrated that the presence of an intramolecular S-Se interaction is mandatory to achieve a high facial selectivity in methoxyselenenylation reactions as well as in cyclofunctionalization reactions.[8]

SBIs are also responsible of the activation of the catalytic site of the glutathione peroxidase, a crucial selenoenzyme responsible for destroying lipid-damaging peroxides in mammalians, protecting the biomembranes from oxidative stress and, consequently, from a number of pathologies.[11] Recent studies demonstrated that intramolecular Se···O or Se···N interactions play an important role in the catalytic antioxidant activity of these compounds.[12] As direct consequence of SBIs, the electrophilicity of the chalcogen atom in an organic scaffold results to be modified, with effects in a series of other biological processes.[13]

All these examples make the deep understanding of the ChB of fundamental importance and, in the last years, an intense research activity aimed to this point.[14] From the computational point of view,

the secondary interactions of chalcogenadiazoles have been already studied with different methods, as the Quantum Theory Atom in Molecule (QTAIM), Natural Bond Orbital (NBO) and Voronoi Deformation Density (VDD).[15]

Recently, Taylor and co-workers synthesized a series of benzotelluradiazoles, with the precise aim to study the ChB between tellurium and Lewis bases in solution.[16] The association constants (K_a) were determined by UV-Vis and ^{1}H NMR titrations in different organic solvents, varying the substituents on the aromatic ring to tune the electronic properties of tellurium (compounds **2-5**,[17] Scheme 1) and different bases, either anionic (chloride, bromide, iodine and nitrate anions) and neutral (quinuclidine, **Q**, Scheme 1).

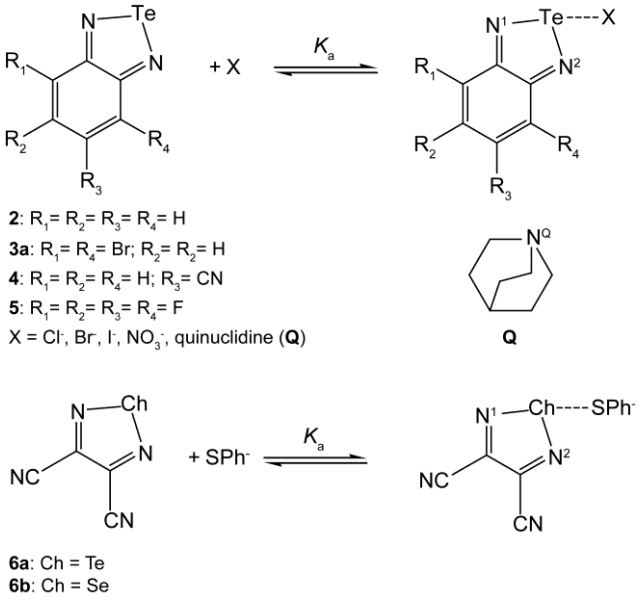

Scheme 1. Formation of chalcogen-bonded adducts and numbering of the species.

The results demonstrated that the substituents R_{1-4} can finely tune the value of K_a, which can reach considerable values in organic solvents (130000 M^{-1} for **5**Cl in THF).[16] Substituting the phenyl moiety with two electrowithdrawing cyanide groups (compounds **6a** and **6b**, Scheme 1) and using the thiophenolate as Lewis base, the group of Beckmann, Gritsan and Zibarev obtained even higher values, reaching 10^8 in THF.[15a]

In this paper, we study the same adducts through the Charge Displacement (CD) analysis,[18] which already demonstrated its potential in the characterization of secondary interactions (frustrated Lewis pairs,[19] hydrogen[20] and halogen bonding[21]) and coordination bonds.[22] Such an approach relies on the integration along a given direction *z* (eq. 1) of the difference of electronic density [$\Delta\rho(x,y,z)$] between the adduct and its non-interacting fragments (in our case the benzotelluradiazole and the Lewis base), frozen in the same positions they occupy in the adduct.

$$\Delta q(z') = \int_{-\infty}^{\infty} dx \int_{-\infty}^{\infty} dy \int_{-\infty}^{z'} dz\, \Delta\rho(x,y,z) \qquad \text{Eq. 1}$$

The value of $\Delta q(z')$ defines the amount of the electronic charge that, upon formation of the adduct, has moved across a plane perpendicular to the axis through the coordinate z'. At the boundary between the fragments (see Computational Detail for the choice of the boundary) the value of Δq is represented by the symbol ω.

To the best of our knowledge, the CD analysis has never been used for the characterization of ChB, but its density-based nature, its stability toward the computational details (in particular the choice of the basis set size and XC functional, see Computational Details) and its propensity to study linear adducts makes it a potentially useful tool.

The results presented here give a detailed and quantitative picture of the ChB between benzotelluradiazoles and Lewis bases, providing also a reliable methodology to predict the value of the free energy of interaction of systems for which experimental data are not available yet.

Results and Discussion

In the optimized structure of **3a**, the molecule shows a C_{2v} symmetry (two mirror planes and one C_2 axis) and the two N-Te distances are both 1.994 Å. The formation of the adduct with the chloride (**3a**Cl) lowers the symmetry to C_s (only one mirror plane containing the whole molecule) because the chloride approaches the tellurium on the opposite side of one of the nitrogen atoms (hereafter called

N^1), where actually the σ-hole[23] is located,[16] forming a N^1-Te-Cl angle of 172.9°. In the adduct **3a**Cl, the N^1-Te distance is considerably longer than in **3a** (2.066 Å), while the N^2-Te bond, roughly perpendicular to the Te···Cl axis, is less affected (2.022 Å) by the interaction with the base.

Visualizing the 3D plot of $\Delta\rho$, it is possible to describe in details the electronic re-organization within the adduct upon the formation of the chalcogen bond (Figure 1).

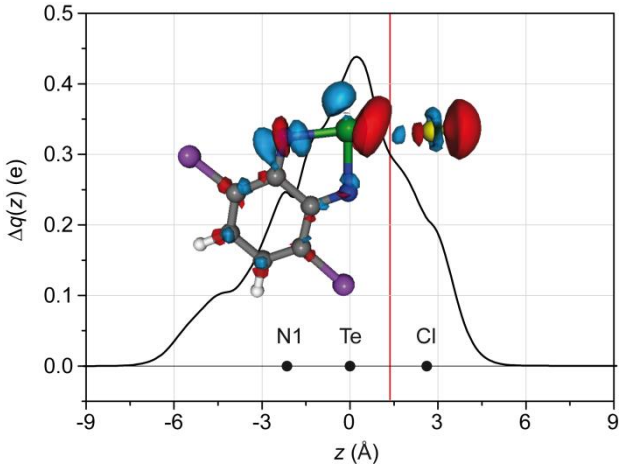

Figure 1. Charge Displacement function for **3a**Cl. The black dots represent the *z* coordinate of the atoms. The red vertical line identifies a suitable boundary between the two fragments. Overprinted: 3D contour plot of the change of electronic density upon formation of the adduct **3a**Cl. Blue (red) isosurfaces identify regions in which the electron density increases (decreases). Density value at the isosurfaces: ±0.003 au.

On the chloride a large depletion of electron density, especially located at the opposite side with respect to the tellurium, and a small ring-shaped accumulation are visible. Between the chloride and the tellurium there is a small electron accumulation, while two large lobes are present on the tellurium. The lobe facing the chloride indicates a marked electron depletion, the other one an electron accumulation. Furthermore, also N^1 shows a remarkable electron accumulation, with a ring-shaped electron depletion around the nucleus. The electron accumulation on N^2 is similar but considerably smaller than that on N^1.

The accumulation/depletion pattern described above depicts a net charge transfer from the chloride to the benzotelluradiazole, as denoted by the electronic accumulation visible in the inter-fragment region. The tellurium atom results to be strongly polarized (as indicated by the two opposite lobes), with the electrons that are repelled by the charge of the anion and accumulate on the other side. But the tellurium is not the ultimate electron density recipient, as evidenced from the accumulation regions on the two nitrogen atoms (on N^1 more than in N^2). Since the N-Te bonds can be described also as a dative bond between an imide anion ($=N^-$) and a dicationic tellurium atom (Te^{2+}), the electron density accumulation region on the nitrogen weakens the bond, which is actually longer than in the case of the isolated molecule.

In order to quantify the electronic flux, $\Delta\rho$ has been integrated along the axis connecting Te and Cl (z) giving the CD function depicted in Figure 1. The CD function is positive throughout the whole molecule, indicating a net charge transfer from the right (chloride) to the left (tellurium) side of the adduct. It can be noted that the flux peaks on the tellurium, but it does not stop on the latter, continuing to be positive until N^1, where it decays to zero. The value of Δq at the inter-fragment boundary (ω) is 0.3 e. As the 3D plot of $\Delta\rho$ revealed, charge transfer and tellurium polarization coexist in the inter-fragment region, therefore the ω value sums up both the contributions. At this stage, the disentaglement between the two is not possible (see later).[23]

Figure 2 shows the same calculations for a neutral adduct, **3aQ**. As it can be seen, the 3D plot is qualitatively similar to that for **3a**Cl (depletion on N^Q, accumulation between N^Q and Te, polarization on Te and accumulation on N^1), with the only difference that the polarization on Te is much smaller with respect to the previous case. This can be explained with the charge of the chloride that repels the electrons of the tellurium to a larger degree than a neutral base.

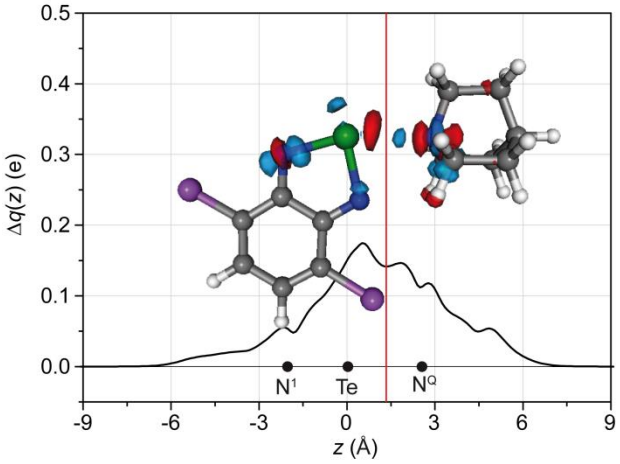

Figure 2. Charge Displacement function for **3aQ**. The black dots represent the *z* coordinate of the atoms. The red vertical line identifies a suitable boundary between the two fragments. Overprinted: 3D contour plot of the change of electronic density upon formation of the adduct **3aQ**. Blue (red) isosurfaces identify regions in which the electron density increases (decreases). Density value at the isosurfaces: ±0.003 au.

The corresponding CD function (Figure 2) is again similar in shape to that for **3a**Cl, but weaker in intensity (ω = 0.141 e). This could be due to the smaller donation properties of **Q** and/or the smaller polarization induced by **Q** with respect to Cl^-. Incidentally, the same difference can be found analyzing the CD curves relative to the halogen bonded adducts $C_6F_5I\cdots Cl^-$ and $C_6F_5I\cdots$**Q** (Figure S8†), for which similar values of ω (0.305 amd 0.126 e, respectively), have been obtained.

It is also interesting to note that in the geometry of **3aQ** one of the bromine bound to the aromatic moiety is located in the inter-fragment region (*z* coordinate = 0.966 Å). **3aQ** is the only adduct in which an atom of the benzotelluradiazole falls in the inter-fragment region and this is because the N^1-Te-N^Q angle in this case is sensibly lower than 180° (162.6°). The consequence can be appreciated in Figure 3, where $\Delta\rho$ is plotted at a density value lower than in Figure 2 (±0.0005 instead of ±0.003 au).

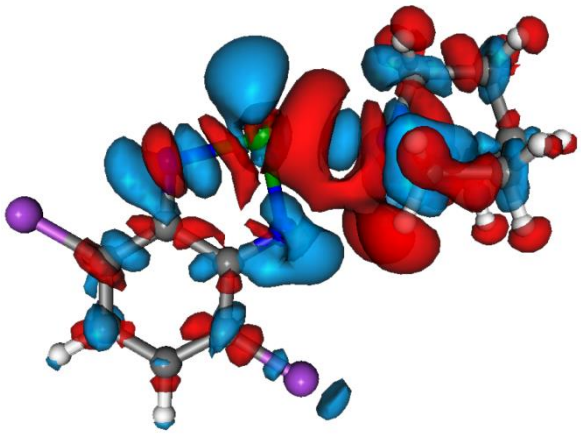

Figure 3. 3D contour plot of the change of electronic density upon formation of the adduct **3aQ**. Blue (red) isosurfaces identify regions in which the electron density increases (decreases). Density value at the isosurfaces: ±0.0005 au.

It is evident that also the bromine in the inter-fragment region undergoes a small electronic re-organization, with the electron flowing from the carbon (electron density depletion) to the bromine (accumulation), therefore in the opposite direction with respect to the flux between the chalcogen and the base. Since ω is the electronic charge that, upon formation of the adduct, has moved across a plane perpendicular to the axis, in the case of **3aQ** ω contains contributions from both the Te ← N and C → Br fluxes.

In all the other adducts the N^1-Te-X angle is closer to 180° and no atoms of the benzotelluradiazoles fall in the inter-fragment region (all the atoms of other benzotelluradiazoles show a *z* coordinate smaller than 0.6 Å). Consequently, **3aQ** is the only one in which the inter-fragment region contains more than one flux.

Expanding the methodology to other Lewis bases, the CD function has been computed for all the **3aX** adducts experimentally studied by Taylor[16] (Figure 4). All of them have the same shape, indicating that the nature of the interaction is similar for all the bases, but there is a trend in the intensities of the functions, which depend on the bond acceptor properties of the base and the magnitude of the polarization.

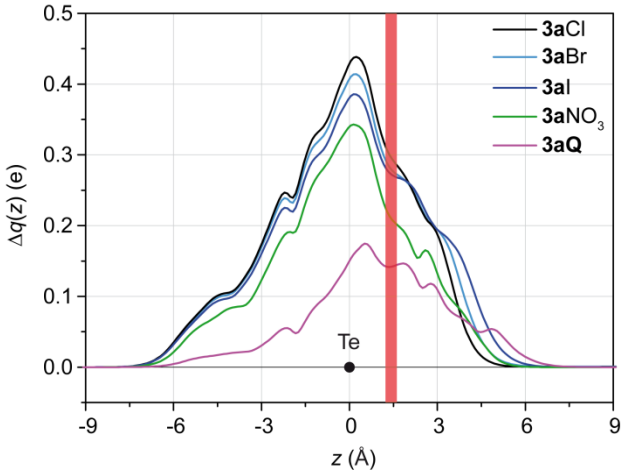

Figure 4. Charge Displacement functions for the **3aX** adducts. The black dot represents the *z* coordinate of the tellurium, always placed at the origin. The red vertical band identifies the range of the inter-fragment boundaries.

The ω values are 0.300, 0.277, 0.269, 0.225 and 0.141 e for **3a**Cl, **3a**Br, **3a**I, **3a**NO_3 and **3aQ**, respectively. The big gap between the ω value of **3aQ** and the others seems an indication of the poor bond acceptor properties of **Q**, but nitrogen-substituted adamantane species (as **Q** or the 1,4-diazabicyclo[2.2.2]octane) showed excellent bond acceptor properties when involved in halogen-bonded adducts.[24] More likely, most of the difference is due to the smaller contribution of the polarization (compare Figure 1 and 2).

In order to take into account the difference between tellurium and selenium adducts, the adducts formed by the structurally similar 3,4-dicyano-1,2,5-chalcogenadiazole and the anion SPh^- (Scheme 1), as experimentally and theoretically characterized by Zibarev and coworkers,[15a] can be compared. The CD curves for the adducts **6a**SPh and **6b**SPh are shown in Figure 5.

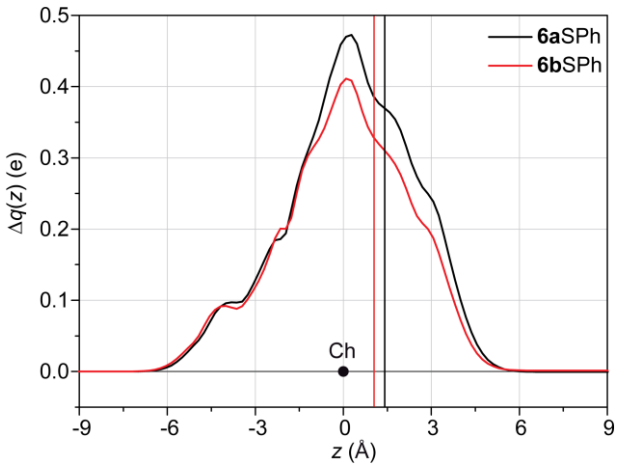

Figure 5. Charge Displacement functions for the **6a**SPh and **6b**SPh adducts, containing tellurium and selenium, respectively. The black dot represents the *z* coordinate of the chalcogen atom, always placed at the origin, while the anion is always placed on the +*z* semiaxis. The black and red vertical lines identifiy the inter-fragment boundaries for **6a**SPh and **6b**SPh, respectively.

Also in this case the shape of the curve is similar to that for **3a**Cl (Figure 1). The values of ω are 0.376 and 0.330 e for **6a**SPh and **6b**SPh, respectively. As expected, the selenium can accept less electronic density with respect to the tellurium, as already stated in the original paper through different methods.[15a] To the best of our knowledge, experimental data are not available for similar systems containing sulfur.

Calculating the value of ω for the adducts for which the K_a has been experimentally evaluated,[25] allows the comparison between ω and the logarithm of the association constants, which is related to the free energy of association (Figure 6). In particular, all the K_a values reported here have been measured in THF by Taylor and co-workers (adducts **2-5X**)[16] or Zibarev and coworkers (**6a-6b**SPh).[15a]

The plot of ω *vs*. ln K_a reveals that if ionic and neutral adducts are treated separately, the two quantities are linearly correlated, with good correlation coefficients (r^2 = 0.9447 and 0.9999 for ionic and neutral adducts, respectively) and similar slopes (m = 0.011 and 0.017 for ionic and neutral adducts,

respectively). **3aQ**, for which, as shown before, the ω values is lowered by the C → Br electronic flux, has been excluded by the fitting procedure.

An alternative way to estimate the charge transfer is the Hirshfeld charge analysis.[26] The latter allows the estimation of the charge on each arbitrarily defined fragment of an adduct, computed as the integral of the adduct electron density over space, weighted at each point by the ratio between the isolated fragment density and the total density of the non-interacting fragments. Using the same fragmentation scheme used for the CD method, the values for the charge transferred from **Q** to **2-5** (q_H) correlate perfectly with ln K_a (Figure 6, r^2 = 0.9916), even including **3aQ** in the fitting procedure. For anionic bases, the the fitting is slightly poorer (r^2 = 0.9177) but still acceptable. In general, q_H shows a very good agreement with the values of ω (Table S1†).

It is interesting to note that **2Q** and **2**NO_3 have the same value of K_a but different values of ω. In addition to this, the polarization contribution in **2Q** is smaller than in **2**NO_3 (see Figure S5 and S6†). Therefore, combining experimental and theoretical data, it seems that the main contribution in determining the K_a value comes from the charge transfer rather than from the polarization. Stretching further the hypothesis, it can be assumed that, in first approximation, only the effective charge transfer (CT_{eff}) is important for the value of K_a. Under this hypothesis, we can consider the values of the intercepts (ω_0) found in the fitting procedure previously described (Figure 6, ω_0 = 0.192 and 0.094 e for ionic and neutral adducts, respectively) as the polarization contributions for neutral and ionic adducts. Now, CT_{eff} can be roughly estimated subtracting the intercept values to ω and goes from 0.02 to 0.18 e for **2**NO_3 and **6a**SPh, respectively, giving the order of magnitude of the "covalent" character of the ChB for these systems.

As shown in Figures 1 and 2, also the N^1-Te bond is affected by the Te···X interaction. Actually, plotting the lengthening of the N^1-Te bond with respect to the isolated benzotelluradiazole *versus* ω, a linear correlation can be appreciated (Figure S7†). In this case there is no differentiation between ionic and neutral adducts, likely because N^1, being far from the Lewis base, is unaffected by the charge of X and because the polarization on Te does not involve the N^1-Te axis (Figure 1).

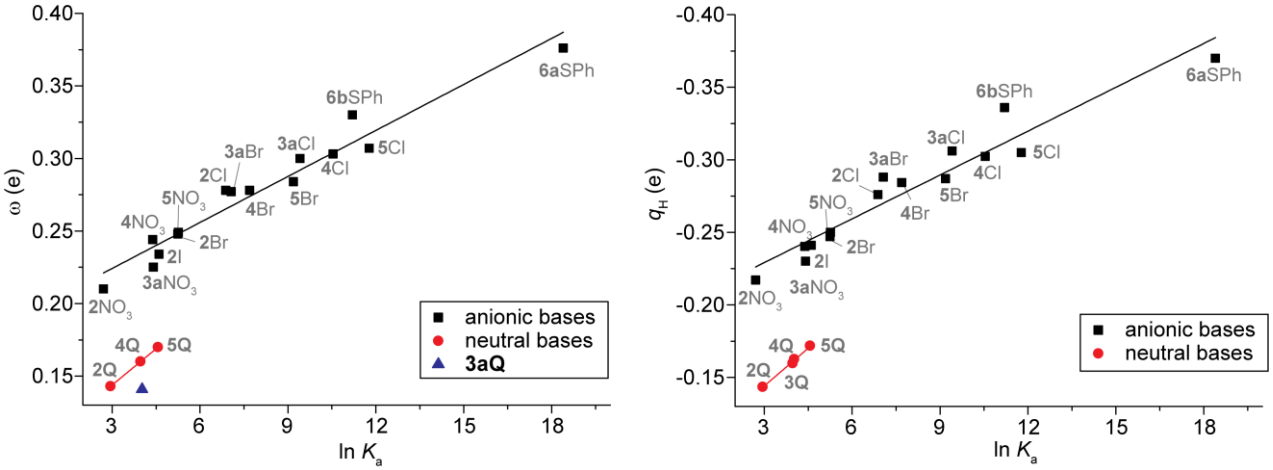

Figure 6. (Left) Linear correlation between ω and the logarithm of the experimental values of K_a. For the exclusion of **3aQ** from the fitting procedure, see the text. (Right) Linear correlation between q_H and the logarithm of the experimental values of K_a.

The goodness of the fitting in Figure 6 suggests that the Charge Displacement analysis can be used as a reliable method to predict the free interaction energy involved in chalcogen bonding for the benzotelluradiazole class of compounds. In fact, the prediction of the association free energy (ΔG^0) computed by B97-D3 calculations (the best XC functional according to the benchmark conducted in ref. 16 and 15a; the solvent effect was taken into account through the PCM model for THF), even if generally acceptable, fails in some cases (see the case of **2Br** or **3a**NO_3 in Figure 7), with a deviation standard of 1.2 kcal/mol and a maximum error of 3.3 kcal/mol. Computing ΔG^0 from the ω value through the fitting equations shown in Figure 6 gives more reliable values (standard deviation = 0.50 kcal/mol, maximum error = 1.0 kcal/mol).[27] Such reliability can be used for the prediction of the ΔG^0 of a chalcogen bonding donor/acceptor couple for which experimental data are missing.

These results open the way to a more reliable theoretical pre-screening for the choice of the optimal donor/acceptor couple. In fact, even if no experimental data were available, the trend of the ΔG^0 values of the adducts would be correctly predicted.

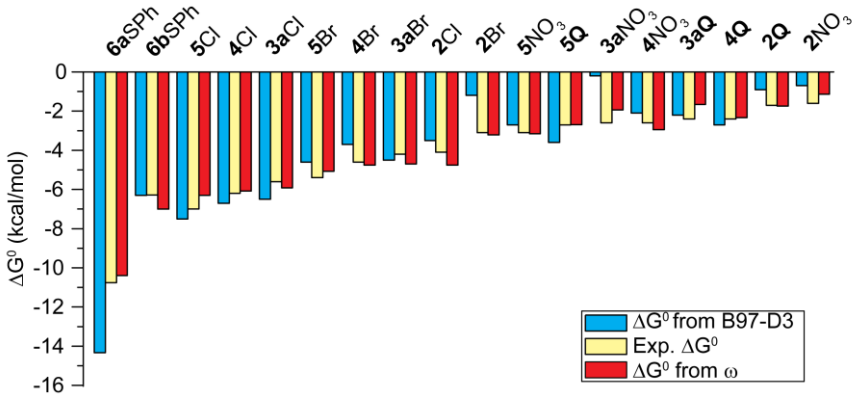

Figure 7. Free energies of chalcogen bonding interactions of **2**X−**6**X. Experimental and B97-D3-computed values are taken from ref. 16 (**2**X-**5**X) and 15a (**6a**SPh and **6b**SPh), ω-computed data are calculated using the proper fitting equation shown in Figure 6.

Conclusions

In this paper, it has been shown that coupling the visual inspection of $\Delta\rho(x,y,z)$ and the Charge Displacement analysis is very useful to describe the interaction between a chalcogen atom and a Lewis base, from both the qualitative and quantitative point of view. Taking into account a series of adducts between substituted benzotelluradiazoles and a series of Lewis bases, either charged and neutral, the corresponding CD functions have always the same general shape, indication that the nature of the Te···X interaction does not depend on the exact nature of the base. The only differences rely on the donor properties of the tellurium and the acceptor properties of the base and, consequently, in the exact value of ω. Moreover, the values of the latter resulted markedly different for neutral and charged bases, since ω contains also a polarization contribution, which is larger for anionic bases. Assuming that the main driving force for the establishment of the ChB is the charge transfer rather than the polarization, the "covalent" character of the interaction can be roughly estimated between 0.02 and 0.18 electrons.

ω values and experimentally-measured ΔG resulted to be linearly correlated, confirming once again the physical likeliness of the CD analysis in describing the formation of adducts bound by weak interactions. Furthermore, once calibrated with experimental data, ω is more reliable than standard

DFT to predict the ΔG of a benzotelluradiazole/base couple for which experimental data are not available. More in general, even if the prediction of the numeric value of ΔG is possible only if a certain number of experimental values are available, the trend of the values can be efficiently predicted even without any experimental values, for instance for new classes of ChB donors, opening the way to a reliable theoretical pre-screening for the choice of the optimal donor/acceptor couple. When the inter-fragment region contains other atoms than those involved in the SBI, as in the case of **3aQ**, the analysis of the Hirshfeld charges can satisfactorily replace the CD method, even without the details that the analysis of the CD functions throughout the whole molecule allows.

Finally, this study demonstrates how the synergistic coupling of theoretical and experimental data can be fruitfully applied to the chalcogen bonding, allowing in the near future to study in detail the nature and the effects of weak interactions in chemically and biologically relevant systems.

Acknowledgements. Instituto de Física da Universidade Federal da Bahia is acknowledged for computational resources, Dr. Sergio Rampino is kindly acknowledged for providing "Cubes", a suite of tools for the manipulation of electronic density matrices. This research was undertaken as part of the scientific activity of the international multidisciplinary "SeS Redox and Catalysis" network.

Corresponding authors

*Email: g.ciancaleoni@ufsc.br

Computational Datails

All thermodynamic calculations were performed using the Gaussian 09 program.[28] All the optimizations ($C_6F_5I\cdots Cl^-$ and $C_6F_5I\cdots$**Q**) were carried out using density functional theory employing B97D3[29] functional, the def2-TZVP basis set and the ECP pseudopotential for iodine,[30] as stored in the Basis Set Exchange portal.[31] All the optimized adducts show only positive vibrations. The geometries for **2-5X** and **6a**SPh and **6b**SPh have been taken from ref. 16 and 15a, respectively, and

used without further reoptimization. When necessary, the geometries have been re-oriented to have the *z* axis passing between the chalcogen atom (origin) and the Lewis base (positive values of *z*).

All the Charge Displacement calculations were carried out using density functional theory employing the BP86[32] corrected for the dispersion, using the Grimme D3-parametrized XC functionals,[33] the def2-TZVP basis set and the ECP pseudopotential for tellurium. The CD method already resulted to be remarkably stable with respect to the exchange-correlation functional employed, the basis set and the level of theory to account the relativistic effects (scalar or full four-component hamiltonian).[22b,22c,34] Here, the CD function has been calculated for **3a**Cl with different XC functionals, giving very similar curves in all the cases (Figure S1†).

In order to characterize the interaction with only one value of Δq, it is useful to fix a plausible boundary separating the fragments in the adducts. We choose the isodensity value representing the point on the *z* axis at which equal-valued isodensity surfaces of the isolated fragments are tangent. At this point the value of Δq is represented by the symbol ω.[22]

References

[1] K. Müller-Dethlefs and P. Hobza, *Chem. Rev.* 2000, **100**, 143-167.

[2] (a) B. M. Goldstein, S. D. Kennedy and W. J. Hemnen, *J. Am. Chem. Soc*. 1990, **112**, 8265-8268; (b) D. H. R. Barton, M. B. Hall, Z. Lin, S. I. Pareck and J. Reibenspies, *J. Am. Chem. Soc*. 1993, **115**, 5056-5059; (c) V. N. Ramasubbu and R. Parthasarathy, *Phosphorus Sulfur Silicon Relat. Elem*. 1987, **31**, 221-229; (d) M. Baiwir, G. Llabres, O. Dideberg, L. Dupont and J.-L. Piette, *Acta Crystallogr., Sect. B* 1975, **31**, 2188-2191; (e) H. W. Roesky, K.- L. Weber, U. Seseke, W. Pinkert, M. Noltemeyer, W. Clegg and G. M. Sheldrick, *J. Chem. Soc., Dalton Trans.* 1985, 565-571; (f) S. Tomoda, M. Iwaoka, K. Yakushi, A. Kawamoto and J. Tanaka, *J. Phys. Org. Chem*. 1988, **1**, 179-184; (g) S. Tomoda and M. Iwaoka, *J. Chem. Soc., Chem. Commun.* 1990, 231-233; (h) S. Kubiniok, W.-Wdu

Mont, S. Pohl and W. Saak, *Angew. Chem. Int. Ed.* 1988, **27**, 431-433; (i) W.-W. du Mont, A. Martens, S. Pohl and W. Saak, *Inorg. Chem*. 1990, **29**, 4847-4848.

[3] I. Caracelli, I. Haiduc, J. Zukerman-Schpector and E. R. T. Tiekink, *PATAI´s Chemistry of Functional Groups* 2014, 1-16, Ed. John Wiley and Sons.

[4] (a) A. F. Cozzolino, I. Vargas-Baca, S. Mansour and A. H. Mahmoudkhani, *J. Am. Chem. Soc*. 2005, **127**, 3184-3190; (b) W. Wang, B. Ji and Y. Zhang, *J. Phys. Chem. A* 2009, **113**, 8132-8135; (c) M. E. Brezgunova, J. Lieffrig, E. Aubert, S. Dahaoui, P. Fertey, S. Labègue, J. G. Ángyán, M. Fourmigué and E. Espinosa, *Cryst. Growth Des.* 2013, **13**, 3283-3289.

[5] D. Manna and G. Mugesh, *J. Am. Chem. Soc.* 2012, **134**, 4269-4279; P. Metrangolo and G. Resnati, *Nat. Chem.* 2012, **4**, 437-438.

[6] M. C. Aragoni, M. Arca, F. A. Devillanova, F. Isaia and V. Lippolis, *Cryst. Growth Des.* 2012, **12**, 2769-2779.

[7] (a) M. Iwaoka and S. Tomoda, *J. Am. Chem. Soc.* 1996, **118**, 8077-8084; (b) M. C. Aragoni, M. Arca, F. A. Devillanova, A. Garau, F. Isaia, V. Lippolis and G. Verani, *Coord. Chem. Rev.* 1999, **184**, 271-290; (c) H. Komatsu, M. Iwaoka and S. Tomoda *Chem. Commun*. 1999, 205–206.

[8] M. Tiecco, L. Testaferri, C. Santi, C. Tomassini, S. Santoro, F. Marini, L. Bagnoli, A. Temperini and F. Costantino, *Eur.J. Org. Chem*. 2006, **21**, 4867-4873.

[9] J. Černý and P. Hobza, *Phys. Chem. Chem. Phys*. 2007, **9**, 5291-5303.

[10] (a) J. M. Williams, J. R. Ferraro, R. J. Thorn, K. D. Carlson, U. Geier, H. H. Wang, A. M. Kini and M.-H. Whangbo, *Organic Superconductors*; Prentice Hall: Englewood Cliffs, NJ, 1992; (b) M. Iwaoka, S. Takemoto, M. Okada and S. Tomoda, *Bull. Chem. Soc. Jpn.* 2002, **75**, 1611-1625.

[11] (a) J. Mukherjee, S. S. Zade, H. B. Singh and R. B. Sunoj, *Chem. Rev.* 2010, **110**, 4357-4416; (b) E. E. Alberto, V. Nascimento and A. L. Braga, *J. Brazil. Chem. Soc.* 2010, **21**, 2032-2041; (c) V. Nascimento, E. E. Alberto, D. W. Tondo, D. Dambrowski, M. R. Detty, F. Nome and A. L. Braga, *J. Am. Chem. Soc.* 2012, **134**, 138-141.

[12] T. Takei, Y. Urabe, Y. Asahina, H. Hojo, T. Nomura, K. Dedachi, K. Arai and M. Iwaoka, *J. Phys. Chem. B* 2014, **118**, 492-500.

[13] (a) C. Santi, C. Tidei, C. Scalera, M. Piroddi and F. Galli, *Curr. Chem. Biol*. 2013, **7**, 25-36; (b) D. Bartolini, J. Commodi, M. Piroddi, L. Incipini, L. Sancineto, C. Santi and F. Galli, *Free Rad. Biol. & Med.* 2015, DOI: 10.1016/j.freeradbiomed.2015.06.039.

[14] (a) J. S. Murray, P. Lane, T. Clark and P. Politzer, *J. Mol. Model.* 2007, **13**, 1033-1038; (b) S. P. Thomas, K. Satheeshkumar, G. Mugesh and T. N. G. Row, *Chem. Eur. J.* 2015, **21**, 6793-6800; (c) J.-L. Zhao, Q.-Z. Li, Z.-B. Liu and J. B. Cheng, *Molecular Physics* 2012, 1-7; (d) M. Iwaoka, H. Komatsu, T. Katsuda and S. Tomoda, *J. Am. Chem. Soc.* 2002, **124**, 1902-1909; (e) P. Ramasami and T. A. Ford, *J. Mol. Model.* 2015, **21**, 35; (f) A. Nordheider, E. Hupf, B. A. Chalmers, F. R. Knight, M. Bühl, S. Mebs, L. Chęcińska, E. Lork, P. S. Camacho, S. E. Ashbrook, K. S. A. Arachchige, D. B. Cordes, A. M. Z. Slawin and J. Beckmann, J. D. Woollins, *Inorg. Chem.* 2015, **54**, 2435-2446.

[15] (a) N. A. Semenov, A. V. Lonchakov, N. A. Pushkarevsky, E. A. Suturina, V. V. Korolev, E. Lork, V. G. Vasiliev, S. N. Konchenko, J. Beckmann, N. P. Gritsan and A. V. Zibarev, *Organometallics* 2014, **33**, 4302-4314; (b) A. F. Cozzolino, P. J. W. Elder, L. M. Lee and I. Vargas-Baca, *Can. J. Chem.* 2013, **91**, 338-347; (c) A. F. Cozzolino, A. D. Bain, S. Hanhan and I. Vargas-Baca, Chem. Commun. 2009, 4043-4045.

[16] G. E. Garrett, G. L. Gibson, R. N. Straus, D. S. Seferos and M. S. Taylor, *J. Am. Chem. Soc.* 2015, **137**, 4126-4133.

[17] The numbering is the same used in the Ref. 16.

[18] L. Belpassi, I. Infante, F. Tarantelli and L. Visscher, *J. Am. Chem. Soc*. 2008, **130**, 1048-1060.

[19] L. Rocchigiani, G. Ciancaleoni, C. Zuccaccia and A. Macchioni, *J. Am. Chem. Soc.* 2014, **136**, 112-115.

[20] E. Ronca, L. Belpassi and F. Tarantelli, *Chemphyschem* 2014, **15**, 2682-2687; D. Cappelletti, E. Ronca, L. Belpassi, F. Tarantelli and F. Pirani, *Acc. Chem. Res.* 2012, **45**, 1571-1580.

[21] D. Cappelletti, A. Bartocci, F. Grandinetti, S. Falcinelli, L. Belpassi, F. Tarantelli and F. Pirani, *Chem. Eur. J.* 2015, **21**, 6234-6240; A. Bartocci, L. Belpassi, D. Cappelletti, S. Falcinelli, F. Grandinetti, F. Tarantelli and F. Pirani, *J. Chem. Phys.* 2015, **142**, 184304.

[22] (a) G. Ciancaleoni, L. Biasiolo, G. Bistoni, A. Macchioni, F. Tarantelli, D. Zuccaccia and L. Belpassi, *Chem. Eur. J.* 2015, **21**, 2467-2473; (b) G. Ciancaleoni, N. Scafuri, G. Bistoni, A. Macchioni, F. Tarantelli, D. Zuccaccia and L. Belpassi, *Inorg. Chem.* 2014, **53**, 9907-9916; (c) G. Bistoni, L. Belpassi and F. Tarantelli, *Angew. Chem., Int. Ed*. 2013, **52**, 11599-11602.

[23] P. Politzer, J. S. Murray and T. Clark, *Phys. Chem. Chem. Phys.* 2013, **15**, 11178-11189.

[24] (a) G. Ciancaleoni, R. Bertani, L. Rocchigiani, P. Sgarbossa, C. Zuccaccia and A. Macchioni, *Chem. Eur. J.* 2015, **21**, 440-447; (b) R. Cabot and C. A. Hunter, *Chem. Commun*. 2009, 2005 –2007; (c) O. Dumele, D. Wu, N. Trapp, N. Goroff and F. Diederich, *Org. Lett.* 2014, **16**, 4722-4725.

[25] The CD functions for other adducts are available as Electronic Supplementary Information, Figure S2-S4 and Table S1.†

[26] F. L. Hirshfeld, *Theor. Chim. Acta* 1977, **44**, 129-138; G. Te Velde, F. M. Bickelhaupt, E. J. Baerends, C. Fonseca Guerra, S. J. A. van Gisbergen, J. G. Snijders and T. Ziegler, *J. Comput. Chem*., 2001, **22**, 931–967.

[27] It is important to underline here that the computation of ω is fast and computationally unexpensive, just requiring the geometry optimization of the adduct and the generation of the matrices (cubes) describing the electronic density of the adduct and the fragments. Post-processing operations consist in the manipulation and integration of such cubes.

[28] M. J. Frisch, G. W. T., H. B. Schlegel, G. E. Scuseria, M. A. Robb, J. R. Cheeseman, G. Scalmani, V. Barone, B. Mennucci, G. A. Petersson, H. Nakatsuji, M. Caricato, X. Li, H. P. Hratchian, A. F. Izmaylov, J. Bloino, G. Zheng, J. L. Sonnenberg, M. Hada, M. Ehara, K. Toyota, R. Fukuda, J. Hasegawa, M. Ishida, T. Nakajima, Y. Honda, O. Kitao, H. Nakai, T. Vreven, J. A. Montgomery, Jr., J. E. Peralta, F. Ogliaro, M. Bearpark, J. J. Heyd, E. Brothers, K. N. Kudin, V. N. Staroverov, T. Keith, R. Kobayashi, J. Normand, K. Raghavachari, A. Rendell, J. C. Burant, S. S.

Iyengar, J. Tomasi, M. Cossi, N. Rega, J. M. Millam, M. Klene, J. E. Knox, J. B. Cross, V. Bakken, C. Adamo, J. Jaramillo, R. Gomperts, R. E. Stratmann, O. Yazyev, A. J. Austin, R. Cammi, C. Pomelli, J. W. Ochterski, R. L. Martin, K. Morokuma, V. G. Zakrzewski, G. A. Voth, P. Salvador, J. J. Dannenberg, S. Dapprich, A. D. Daniels, O. Farkas, J. B. Foresman, J. V. Ortiz, J. Cioslowski, and D. J. Fox,, Gaussian 09, Gaussian, Inc., Wallingford CT, 2013.

[29] S. Grimme, S. Ehrlich, L. Goerigk, *J. Comput. Chem.*, 2011, **32**, 1456-65.

[30] (a) F. Weigend, R. Ahlrichs, *Phys. Chem. Chem. Phys*., 2005, **7**, 3297-3305; (b) K. A. Peterson, D. Figgen, E. Goll, H. Stoll and M. Dolg, *J. Chem. Phys*., 2003, **119**, 11113.

[31] K. L. Schuchardt, B. T. Didier, T. Elsethagen, L. Sun, V. Gurumoorthi, J. Chase, J. Li and T. L. Windus, *J. Chem. Inf. Model*. 2007, **47**, 1045-1052.

[32] A. D. Becke, *Phys. Rev. A* 1988, **38**, 3098-3100; J. P. Perdew, *Phys. Rev. B* 1986, **33**, 8822-8824.

[33] S. Grimme, J. Antony, S. Ehrlich and H. Krieg, *J. Chem. Phys.* 2010, **132**, 154104.

[34] K. M. Azzopardi, G. Bistoni, G. Ciancaleoni, F. Tarantelli, D. Zuccaccia and L. Belpassi, *Dalton Trans.* 2015, **44**, 13999-14007.